

pubs.acs.org/JACS Article

# NEIL1 Recoding due to RNA Editing Impacts Lesion-Specific Recognition and Excision

Elizabeth R. Lotsof, Allison E. Krajewski, Brittany Anderson-Steele, JohnPatrick Rogers, Lanxin Zhang, Jongchan Yeo, Savannah G. Conlon, Amelia H. Manlove, Jeehiun K. Lee, and Sheila S. David



Cite This: J. Am. Chem. Soc. 2022, 144, 14578-14589



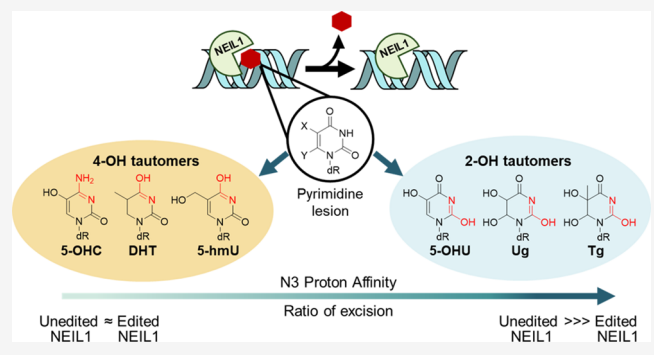
**ACCESS** I

III Metrics & More

Article Recommendations

Supporting Information

ABSTRACT: A-to-I RNA editing is widespread in human cells but is uncommon in the coding regions of proteins outside the nervous system. An unusual target for recoding by the adenosine deaminase ADAR1 is the pre-mRNA of the base excision DNA repair enzyme NEIL1 that results in the conversion of a lysine (K) to arginine (R) within the lesion recognition loop and alters substrate specificity. Differences in base removal by unedited (UE, K242) vs edited (Ed, R242) NEIL1 were evaluated using a series of oxidatively modified DNA bases to provide insight into the chemical and structural features of the lesion base that impact isoform-specific repair. We find that UE NEIL1 exhibits higher activity than Ed NEIL1 toward the removal of oxidized



pyrimidines, such as thymine glycol, uracil glycol, 5-hydroxyuracil, and 5-hydroxymethyluracil. Gas-phase calculations indicate that the relative rates in excision track with the more stable lactim tautomer and the proton affinity of N3 of the base lesion. These trends support the contribution of tautomerization and N3 protonation in NEIL1 excision catalysis of these pyrimidine base lesions. Structurally similar but distinct substrate lesions, 5-hydroxycytosine and guanidinohydantoin, are more efficiently removed by the Ed NEIL1 isoform, consistent with the inherent differences in tautomerization, proton affinities, and lability. We also observed biphasic kinetic profiles and lack of complete base removal with specific combinations of the lesion and NEIL1 isoform, suggestive of multiple lesion binding modes. The complexity of NEIL1 isoform activity implies multiple roles for NEIL1 in safeguarding accurate repair and as an epigenetic regulator.

# ■ INTRODUCTION

The integrity of DNA is compromised by nucleobase oxidation due to reactive oxygen and nitrogen species (RONS) formed via endogenous and exogenous processes. A primary means to repair oxidatively damaged DNA bases is the base excision repair (BER) pathway. DNA glycosylases initiate BER by the identification of aberrant DNA bases and catalyzing Nglycosidic bond hydrolysis of the damaged nucleotide or its inappropriately placed partner.<sup>2</sup> Unrepaired DNA nucleobase modifications lead to mutagenesis and genomic instability that contribute to diseases, such as cancer, accelerated aging, and neurodegeneration.<sup>3</sup> In addition, a variety of metabolic syndromes are associated with the loss or variants of DNA glycosylases, such as NEIL1, OGG1, and NTHL, have been observed in knock-out mice models. 4-6 The loss of NEIL1 has also been associated with immune deficiencies, Alzheimer's disease,8 and impaired memory retention.5

NEIL1 is unique among BER glycosylases due to the presence of two distinct isoforms resulting from editing of the NEIL1 pre-mRNA by the adenosine deaminase ADAR1 (Figure 1C). 10-12 Specifically, the adenosine (A) at position 725 in the NEIL1 pre-mRNA is converted to inosine (I) by

ADAR1.<sup>12</sup> Since inosine codes as guanosine (G) during translation, the edited mRNA codes for an arginine (R) at position 242 in NEIL1 rather than the lysine (K) coded in the unedited mRNA. Dramatic alterations in lesion removal activity result from the single amino acid change between the unedited (UE, K242) and edited (Ed, R242) NEIL1 isoforms.<sup>12</sup> Specifically, UE NEIL1 removes thymine glycol (Tg) in duplex DNA about ~30- to 40-fold faster than Ed NEIL1.<sup>12</sup> Structural studies of Ed and UE NEIL1 bound to a Tg duplex showed that the Lys242 or Arg242 side chain, within the lesion recognition loop of NEIL1, interacts with the Tg base.<sup>13</sup> However, the two isoforms exhibited similar affinity in electrophoretic mobility shift assays (EMSAs) to duplex DNA-containing noncleavable synthetic analogues, 2'-fluorothymidine glycol (FTg) and 2'F-guanidinohydantoin

Received: April 4, 2022 Published: August 2, 2022





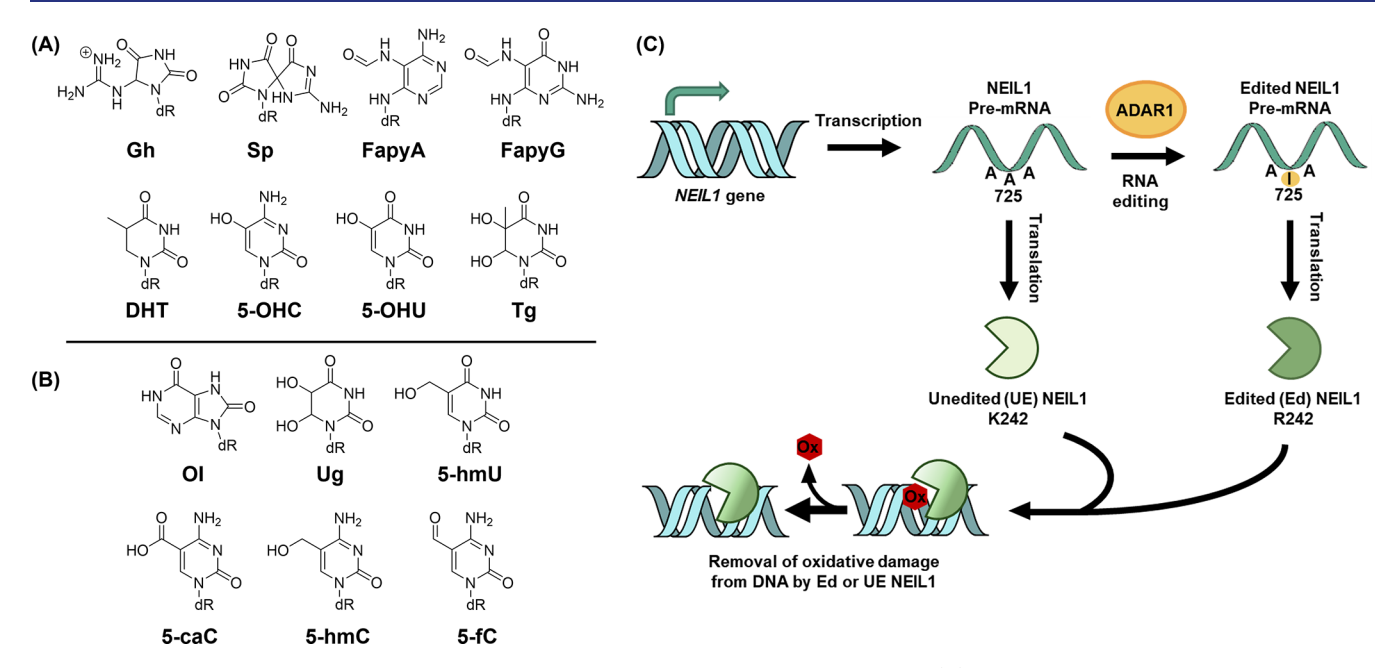


Figure 1. Base lesions evaluated for removal by NEIL1 isoforms produced by RNA editing. (A) Known substrates for edited NEIL1: Gh, guanidinohydantoin; Sp, spiroiminodihydantoin; FapyA, 4,6-diamino-5-formamidopyrimidine; FapyG, 2,6-diamino-4-hydroxy-5-formamidopyrimidine; DHT, dihydrothymine; 5-OHC, 5-hydroxycytosine; 5-OHU, 5-hydroxyuracil; Tg, thymine glycol. (B) Additional lesions tested as potential substrates for edited and unedited NEIL1 in this work: OI, 8-oxoinosine; Ug, uracil glycol; 5-hmU, 5-hydroxymethyluracil; 5-caC, 5-carboxycytosine; 5-hmC, 5-hydroxymethylcytosine; 5-fC, 5-formylcytosine. (C) NEIL1 gene encodes for a lysine at position 242 in the NEIL1 enzyme. However, ADAR1 deamination of adenosine 725 to inosine in the NEIL1 pre-mRNA produces anarginine codon at position 242 of NEIL1. Both isoforms of NEIL1 are active and remove the oxidative damage from DNA.

(FGh).<sup>14,15</sup> These results suggested that the origin of the differential lesion processing is related to a kinetic step rather than lesion binding affinity. The biological implications of NEIL1 recoding have not been fully elaborated; however, conspicuously, multiple myeloma cells overexpressing Ed NEIL1 proliferated at significantly higher rates and presented hallmark signatures associated with unrepaired double-strand breaks.<sup>16</sup>

The NEIL1 glycosylase has the remarkable ability to excise a wide array of oxidized purines and pyrimidines.<sup>17</sup> Known substrates for NEIL1 include the hydantoin lesions, guanidinohydantoin (Gh) and spiroiminodihydantoin (Sp), thymine glycol (Tg), 5-hydroxycytosine (5-OHC), 5-hydroxyuracil (5-OHU), dihydrothymine (DHT), and the formamidopyridines (FapyG and FapyA) (Figure 1A). 18-22 NEIL1 is also capable of excising larger alkylation products, such as methyl-FapyG, 8,9-dihydro-8-(2,6-diamino-4-oxo-3,4-dihydropyrimid-5-yl-formamido)-9-hydroxyaflatoxin B<sub>1</sub> (AFB<sub>1</sub>-FapyG), and psoralen-induced cross-links.<sup>23</sup> NEIL1 has also been implicated in epigenetic gene regulation via interactions with further oxidized products of 5-methylcytosine (5-mC), 5formylcytosine (5-fC), and 5-carboxycytosine (5-caC); however, there is conflicting data on the extent that these base modifications serve as NEIL1 substrates (Figure 1B).<sup>24-26</sup> Notably, 8-oxo-7,8-dihydroguanine (OG)<sup>18,27</sup> is not efficiently removed by NEIL1.19 In contrast, the further oxidation products of OG, Gh and Sp, are among the best-documented substrates of NEIL1. 19 In addition, NEIL1 has been shown to remove Gh and Sp in duplex, single strand, bubble, and bulge DNA structures, and G-quadruplexes. 19,28

To uncover the impact of RNA editing on mitigating responses to DNA modifications, we evaluated the kinetics of the glycosylase activity of the two isoforms on substrates previously examined only with Ed NEIL1, such as 5-OHC, 5-

OHU, and DHT and the epigenetic bases 5-hmU, 5-fC, 5-hmC, and 5-caC. We also evaluated uracil glycol (Ug) as a potential NEIL1 substrate due to its structural similarity to Tg and 5-OHU. Ug is a common product of oxidative stress formed by the oxidation and deamination of cytosine (C) and ultimately mediates cytosine-to-thymine (T) transition mutations. <sup>29-31</sup> A human glycosylase had not been previously documented to excise Ug; however, the similarity of NEIL1 to formamidopyrimidine (Fpg) and Nei DNA glycosylases, which are known to excise Ug, suggested NEIL1 as a likely contender (Figure 1B). <sup>30,31</sup> We also evaluated the removal of a modified version of OG, lacking the 2-amino group (8-oxoinosine, OI) by NEIL1 to illuminate the impact of structural modifications on isoform-specific excision.

Our results presented in this study reveal the distinct lesionspecific removal activity of Ed and UE NEIL1. Specifically, we found that several lesions structurally similar to Tg were removed differentially by the two isoforms, with the experimental trend in the UE/Ed excision Tg > Ug > 5- $OHU > 5-hmU \ge DHT > 5-OHC$ . Calculations to reflect the intrinsic properties of the nucleobases, such as the most stable tautomer, N1-H acidity, and N3 proton affinity, provided insight into the features that lead to the differential recognition and excision by the two isoforms. We also observed biphasic kinetics and reduced levels of the overall removal for specific lesions that provides evidence for multiple base binding modes. Identity of the lesion, NEIL1 isoform, and base pairing context all influence the rates and extent of lesion removed. Taken together, the complexity of lesion-specific differences in substrate recognition and excision due to NEIL1 recoding provides insight into the potential biological consequences of this unusual ADAR1-mediated control over DNA repair.

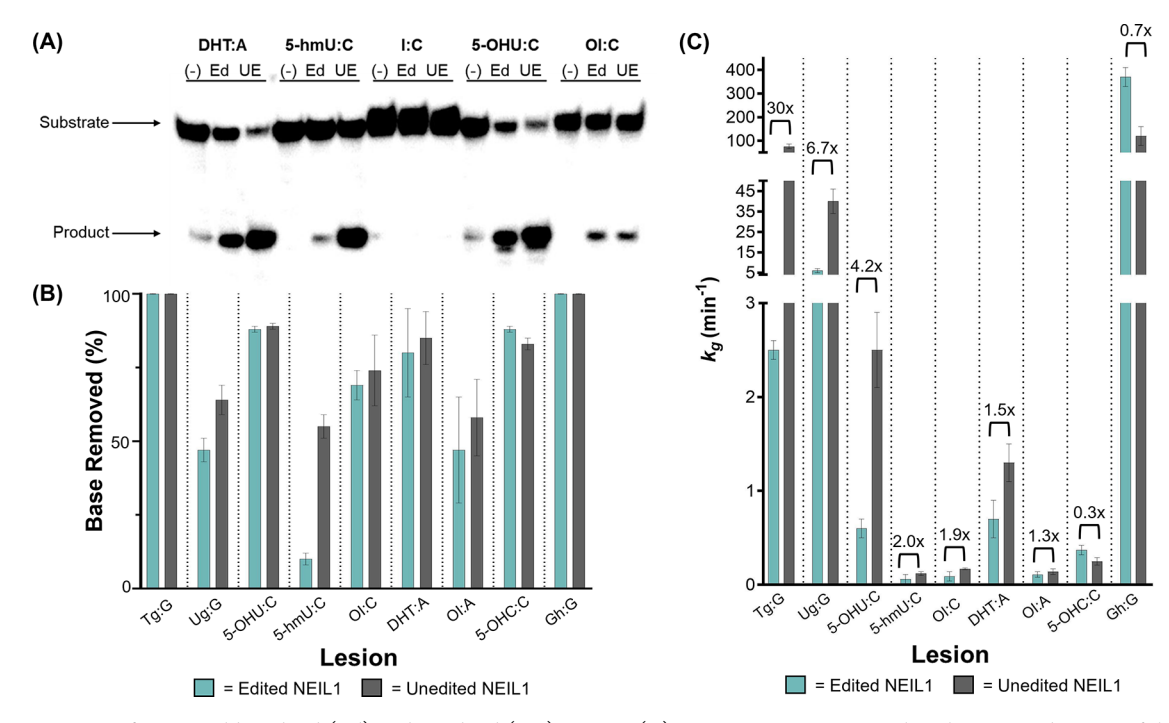


Figure 2. Lesion-specific removal by edited (Ed) and unedited (UE) NEIL1. (A) Representative storage phosphor autoradiogram of the extent of glycosylase activity of Ed (blue) and UE (gray) NEIL1 (200 nM) with DHT:A, 5-hmU:C, I:C, 5-OHU:C, and OI:C-containing 30-bp duplexes (1·2, 20 nM) at 60 min at 37 °C. Modified base removal and strand scission on the duplex substrate lead to a shorter product strand that can be detected via denaturing PAGE. (B) Differences in lesion excision rates ( $k_g$ ) measured under single-turnover conditions with Ed and UE NEIL1 with a variety of lesions (values listed in Table 1). Values above bar represent the ratio of UE/Ed NEIL1 excision for each lesion. (C) Overall extent of base removed (%) by NEIL1 isoforms with various lesions (values listed in Table 1). The lesion-containing DNA duplex substrate (20 nM) was incubated with excess Ed or UE NEIL1 (200 nM) at 37 °C in pH 7.6 buffer containing 150 mM NaCl. The maximal base removed (%) was calculated by dividing the concentration of product produced after a 1 h reaction by the total concentration of the substrate and multiplying by 100. Error bars are the standard deviation for the end point across three trials.

Table 1. Comparison of Lesion Removal Activity from Duplex DNA (1.2) by Edited (Ed) and Unedited (UE) NEIL1

lesion	edited $k_{\rm g}$ , min <sup>-1</sup> (% completion) <sup>a,b</sup>	unedited $k_{\rm g}$ , ${\rm min}^{-1}$ (% completion) $^{a,b}$	$k_{\mathrm{g}}~\mathrm{UE}/k_{\mathrm{g}}~\mathrm{Ed}$
Tg:G <sup>d</sup>	$2.5 \pm 0.1$	$76 \pm 10$	30
Ug:G	6 ± 1 (47%)	$40 \pm 6 \ (64\%)$	6.7
5-OHU:C <sup>e</sup>	$0.6 \pm 0.1 \ (80\%)$	$2.5 \pm 0.4 (83\%)$	4.2
5-hmU:C	$0.06 \pm 0.05 (<10\%)^{c}$	$0.12 \pm 0.02 (55\%)$	2.0
OI:C	$0.09 \pm 0.01 (69\%)$	$0.17 \pm 0.05 (74\%)$	1.9
DHT:A	$0.7 \pm 0.2 \ (81\%)$	$1.3 \pm 0.2 \ (84\%)$	1.5
OI:T	$0.11 \pm 0.03 (47\%)$	$0.14 \pm 0.03 (58\%)$	1.3
5-OHC:C	$0.37 \pm 0.05 (89\%)$	$0.25 \pm 0.04 \ (88\%)$	0.7
$Gh:G^d$	$370 \pm 40$	$120\pm40$	0.3

<sup>&</sup>quot;Rate constants of base removal were measured under single-turnover conditions (20 nM substrate, 200 nM enzyme) at 37 °C (see methods for details of assay conditions). Data was fit to a single-exponential equation,  $P = A(1 - \exp(-k_g t))$ . The percent completion of reactions that did not go to 100% is reported in parentheses. The overall extent of product formation was very low such that the fitting is likely an overestimate of the rate. This data was previously reported in ref 33.

# ■ RESULTS AND DISCUSSION

**Ed and UE NEIL1 Display Distinct Lesion-Specific Removal Activity.** We analyzed the glycosylase activity of NEIL1 on a variety of modified base-containing DNA duplexes (Figure 1) to reveal potential differences in activity arising from the single amino acid difference at position 242, Lys (UE) vs Arg (Ed). The majority of previous analyses of lesion removal have been with Ed NEIL1 due to the original isolation of cDNA from cells where the NEIL1 pre-mRNA had been fully edited. The glycosylase activity of UE and Ed NEIL1 on lesion-containing duplexes in the most likely biological context was initially surveyed by incubating with enzymes in excess for 60 minutes (Table S1 and Figures 2 and

S1). 19,33 Several potential and previously identified NEIL1 substrates were not efficiently removed in our assays. Specifically, U and I are not substrates for either isoform of NEIL1 (Figure S1) and OG, 5-fC, 5-caC, and 5-hmC were removed at extremely low levels by both isoforms (<10%) (Figure S1).

The lack of significant activity of either NEIL1 isoform with the oxidized products of 5-mC, 5-fC, 5-hmC, and 5-caC is surprising in light of previous reports. The detection of NEIL1 in lesion-specific pull-down assays may be due to the interaction of NEIL1 with other proteins that are bound to the epigenetic bases, rather than a direct interaction of NEIL1 with the lesion. The lesions 5-caC and 5-fC are excised by the DNA

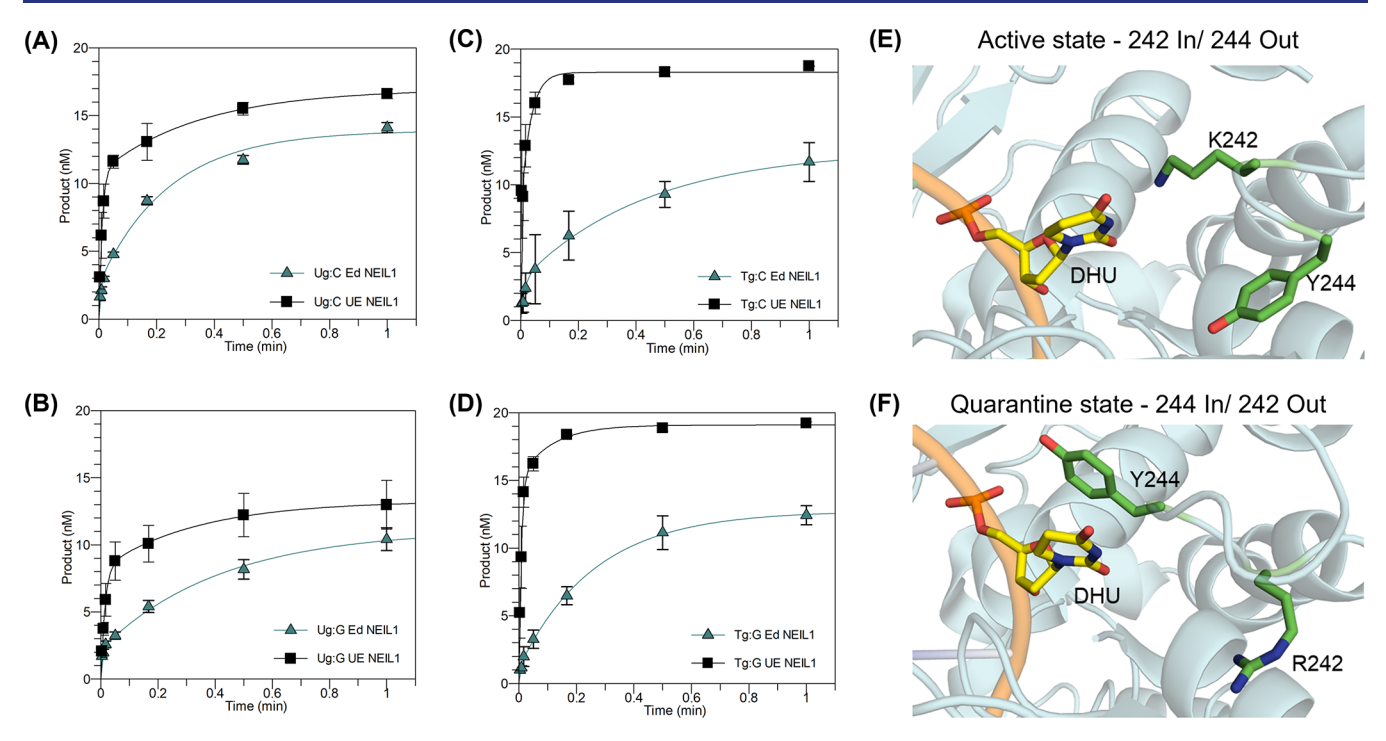


**Figure 3.** Lesion-specific removal of uracil glycol vs thymine glycol demonstrates that small differences in lesion structure dramatically impact base excision by NEIL1 isoforms. Activities of edited (Ed) and unedited (UE) NEIL1 toward duplexes (1•2) containing Ug or Tg were evaluated using rapid quench flow methods with Ed (blue) and UE (black) NEIL1 (200 nM) with a DNA duplex (20 nM) containing (A) Ug:C, (B) Ug:C, (C) Tg:C, and (D) Tg:G at 37 °C with 150 mM NaCl. Data was fit to a two-exponential equation  $P = A(1 - \exp(-k_g 't)) + B(1 - \exp(-k_g 't))$ . (E,F) Alternative conformations of residues 242 and 244 of NEIL1 isoforms were observed with dihydrouracil (DHU) in X-ray structures:UE (K242, PDB ID: 6LWJ) NEIL1 show residue 242 engaged with DHU lesion in an active conformation (E); Ed (R242, PDB ID: 6LWK) NEIL1 show residue 242 away from the DHU lesion and Tyr244 in a proposed quarantine state (F).

glycosylase TDG, <sup>34,35</sup> and NEIL1 has been shown to stimulate TDG turnover. <sup>25,26</sup> Alternatively, the epigenetic C lesions may be converted to other lesions such as 5-hmU that are substrates for NEIL1 or are simply bound but not processed (Figure 2A).

The lesions 5-hmU, 5-OHC, OI, DHT, and 5-OHU were found to be excised to different extents by the NEIL1 isoforms (Figure 2). Minimal excision of 5-hmU was observed when paired with G (<10%); however, in a duplex positioned across from C, 5-hmU was removed to a significant extent by UE NEIL1 (Figure 2B). Similarly, 5-OHC was removed to a small extent by both NEIL1 isoforms (<10%) in a duplex context opposite G but was found to be completely removed when paired with C (Figure S1). Both isoforms removed OI opposite C to similar extents under these conditions. DHT:A, 5-OHU:C, and 5-OHC:C substrates were processed almost completely by Ed and UE NEIL1 in the 60 min incubation period (Figure 2A,B). Based on these observed results, full time course, single-turnover analyses were performed to reveal potential isoform and lesion-specific activity differences (Table 1).

Lack of the 2-Amino-Group in OG Leads to Enhanced Removal by Ed and UE NEIL1. The glycosylase assays revealed that OI is removed, albeit modestly, by both Ed and UE NEIL1 (Figure 2). Full time course glycosylase assays performed under single-turnover conditions ([NEIL1] > [DNA]) with OI duplex substrates paired opposite C and T were fitted to a single-exponential curve to isolate the overall rate constant for glycosidic bond cleavage  $(k_g)$  (Figure 2 and Table 1).  $^{12,19}$  The rate constant  $(k_g)$  for NEIL1 isoformmediated OI removal across C and T indicated a greater activity with UE NEIL1 (1.5–1.9-fold). In addition, UE

NEIL1 was able to effectively remove OI to a slightly higher overall extent relative to the Ed isoform in both duplex contexts (Figure 2 and Table 1). The observation of OI as a substrate is surprising since I and OG are not viable substrates for either isoform. While OI is not a naturally occurring base modification, this allowed us to identify structural features that influence excision by NEIL1. The lack of NEIL1-mediated cleavage of OG has been suggested to be due to the inability of OG to fit within the shallow base binding pocket with fewer hydrogen-bonding interactions and greater solvent exposure.<sup>36</sup> This suggests that the absence of the 2-amino group allows OI to be accommodated more readily in the NEIL1 active site. Notably, the NEIL1 isoforms differ in the extents of OI removal, indicating a distinct impact of the residue at position 242 (Lys > Arg) and opposite base (C > T) on the catalytic placement of OI base within the active site.

**NEIL1 Isoform-Specific Differences in the Removal of 5-hmU, DHT, 5-OHU, and 5-OHC.** The substrate specificity screening (Figures 2A and S1) revealed isoform-specific differences in the removal of pyrimidine lesions. We previously showed the preferred removal of 5-OHU by UE NEIL1 in duplex DNA paired opposite G and C. The help with C, UE NEIL1 removed 5-OHU 4-fold faster ( $k_{\rm g}=2.5\pm0.3~{\rm min}^{-1}$ ) than Ed NEIL1 ( $k_{\rm g}=0.6\pm0.1~{\rm min}^{-1}$ ) (Figure 2 and Table 1). With the DHT:A substrate duplex, UE NEIL1 removed DHT approximately 2-fold faster ( $k_{\rm g}=1.3\pm0.2~{\rm min}^{-1}$ ) than Ed NEIL1 ( $k_{\rm g}=0.7\pm0.2~{\rm min}^{-1}$ ). In addition, DHT removal did not reach completion and the end points were similar for both isoforms. In the case of 5-hmU:C duplex, 5-hmU is removed to high levels by UE NEIL1, despite the fact that the observed

Table 2. Kinetic Parameters from Two-Exponential Fitting of Ug and Tg Removal from Duplex DNA (1•2) by Edited (Ed) and Unedited (UE) NEIL1

			edited			unedited	
duplex	rate co	$nstant (min^{-1})^a$	amplitude $(nM)^b$	completion $(\%)^c$	rate constant (min <sup>-1</sup> ) <sup>a</sup>	amplitude (nM) <sup>b</sup>	completion (%) <sup>c</sup>
Ug:C	$k_{\mathrm{g}}{}'$	$380 \pm 200$	$2.2 \pm 0.4$	$70 \pm 6$	$120 \pm 10$	$10.6 \pm 1.0$	$85 \pm 3$
	$k_g^{"}$	$3.6 \pm 1.0$	$11.5 \pm 0.7$		$3.9 \pm 1.5$	$6.1 \pm 0.6$	
Ug:G	$k_{\mathrm{g}}{}'$	$330 \pm 85$	$2.2 \pm 0.1$	$55 \pm 5$	$68 \pm 10$	$8.8 \pm 1.1$	$73 \pm 8$
	$k_{ m g}{''}$	$2.3 \pm 0.2$	$9.0 \pm 0.9$		$2.8 \pm 1.0$	$5.8 \pm 0.9$	
Tg:C	$k_{ m g}{}'$	>500	$1.2 \pm 0.6$	$58 \pm 3$	$161 \pm 60$	$12.0 \pm 2.1$	$93 \pm 5$
	$k_{ m g}{''}$	$2.9 \pm 0.3$	$11.2 \pm 1.2$		$10 \pm 2$	$5.7 \pm 1.0$	
Tg:G	$k_{ m g}{}'$	>500	$1.3 \pm 0.4$	$62 \pm 5$	$126 \pm 30$	$15.5 \pm 1.1$	$95 \pm 4$
	$k_{\rm g}{''}$	$3.6 \pm 0.1$	$11.6 \pm 0.2$		$7.4 \pm 2$	$3.6 \pm 1.1$	

<sup>&</sup>quot;Data for Ug and Tg removal by Ed and UE NEIL1 fits to a two-exponential equation  $P = A(1 - \exp(-k_g't)) + B(1 - \exp(-k_g''t))$  using a Kintek RQF-3 rapid-quench with 20 nM substrate and 200 nM enzyme at 37 °C. The amplitude (nM) of A and B relates to the associated amplitude and the amount of substrate processed with each rate constant. The overall extent of reaction completion (%) =  $[(A + B)/20 \times 100]$ .

rate constant  $(k_g)$  is significantly smaller than with the DHT, 5-OHU, and Tg substrates (Figure 2 and Table 1).

Our results with 5-OHC underscore the importance of lesion structure and context on NEIL1 isoform activity differences. Minimal removal was observed with 5-OHC across G by both isoforms. Removal of 5-OHC when paired with C in duplex DNA was faster by Ed NEIL1 ( $k_g = 0.37 \pm$  $0.05 \text{ min}^{-1}$ ) over UE NEIL1 ( $k_g = 0.25 \pm 0.04 \text{ min}^{-1}$ ) and reached completion. The observed minimal removal of 5-OHC from the 5-OHC:G duplex was surprising in light of MS studies with  $\gamma$ -irradiated calf thymus DNA where 5-OHC removal was detected by both forms of NEIL1, with higher efficiency with Ed NEIL1.<sup>23</sup> Presumably, features of high MW DNA, such as increased extents of nonspecific DNA and diversity of lesion sequence context, may facilitate 5-OHC removal from 5-OHC:G bps. Remarkably, the isoform specificity with 5-OHC is switched relative to U/T lesions (5-OHU, Tg) with Ed NEIL1 exhibiting higher excision activity (Figure 2 and Table 1). These results further underscore the plasticity of NEIL1 lesion binding modes to adjust to the specific structural features of a given lesion.

Uracil Glycol (Ug) Is More Efficiently Removed by UE **NEIL1.** The Tg lesion exhibited the largest difference in removal by UE relative to Ed NEIL1 (Table 1). To test Ug as a potential substrate, Ug-containing oligonucleotides were prepared (Figure S2).<sup>38</sup> Ug removal under single-turnover conditions by Ed and UE NEIL1 was evaluated using manual (Figure S3) or rapid quench flow methods (Figure S4)<sup>19</sup> and revealed clear isoform-specific differences in Ug removal from Ug:G and Ug:C substrates. The data was fitted to a singleexponential equation to extract  $k_g$  and compared to results with Tg (Table 1 and Figures 2 and S4). For the Ug:G substrate, UE NEIL1 displays a 6-fold faster rate for Ug removal compared to Ed NEIL1. Yet, UE NEIL1 showed a 30-fold faster rate for the removal of Tg from the corresponding Tg:G duplex than Ed NEIL1.12 The smaller difference in relative processing between the two forms is a consequence of both an increased rate of removal of Ug relative to Tg by Ed NEIL1 and a decreased rate of removal of Ug relative to Tg by UE NEIL1. Remarkably, the lack of the single methyl group in Ug results in more similar processing of this lesion by the two NEIL1 isoforms.

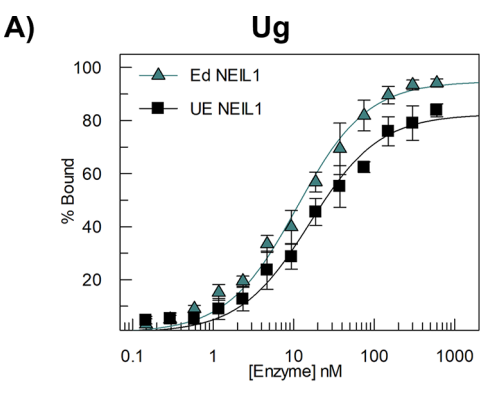
Biphasic Ug Excision by NEIL1 Isoforms Consistent with Multiple Lesion Binding Modes. A feature that emerged in the analysis of Ug removal was that the data was best fit to a two-exponential equation  $P = A(1 - \exp(-k_g't)) + \exp(-k_g't)$ 

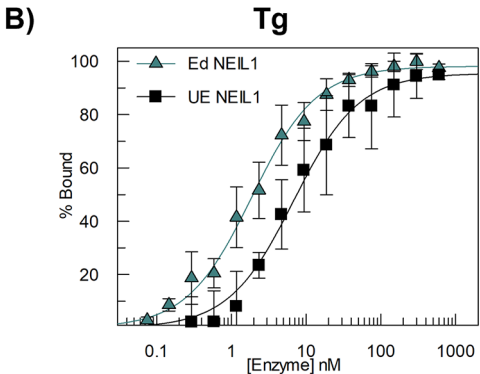
 $B(1 - \exp(-k_g''t))$  (Figure 3) consistent with two distinct excision processes. Though not as visually obvious, the Tg data also was better fitted using a two-exponential equation. In addition, both isoforms remove Ug at overall lower levels of completion relative to Tg (Table 2). The kinetic parameters determined using two-exponential fitting provided a larger rate constant  $(k_g)$  and an associated amplitude, A, and a smaller rate constant  $(k_g'')$  with an associated amplitude, B. We suggest that the two rate constants correspond to two distinct processes where the large rate constant  $k_{\mathrm{g}}{}'$  is associated with lesion removal from the fraction of the lesion bound in a catalytically competent complex, while the smaller rate constant is due to the lesion being positioned in an alternative orientation that requires enzyme/DNA conformational changes for catalysis to take place. The reduced extent of reaction completion with Ug, and several other lesions, suggests a potential third population of lesion that is oriented in a manner that is even less efficiently removed. The ability of NEIL1 to bind lesions in alternative noncatalytically competent conformations is consistent with the recent structural work by Yi and co-workers with Ed and UE NEIL1 bound to several lesion-containing substrates.<sup>39</sup> Two distinct lesion conformations were observed that were dependent on lesion and NEIL1 isoform: the two lesion binding modes were proposed to represent an activated state poised for catalysis and a "quarantine" state that stalls base excision (Figure 3E,F).<sup>39</sup>

A comparison of the Ug and Tg excision rate constants and associated amplitudes provides further insight into the influence of the lesion and NEIL1 isoform on the relative population of the different lesion complexes. Notably, the rate constants  $(k_{\rm g}{}'$  and  $k_{\rm g}{}'')$  for Tg and Ug lesion excisions were overall quite similar for both isoforms of NEIL in all of the base-pairing contexts evaluated (Table 2). However, the associated amplitudes of the two rate constants differ significantly between the two isoforms of NEIL1. For UE NEIL1, the majority of Tg and Ug lesion excisions is associated with the larger rate constant  $(k_g)$  (Figure 3 and Table 2). In contrast with Ed NEIL1, most of the Ug or Tg excision (80-90%) was associated with the smaller rate constant  $(k_{\mathfrak{g}}'')$ . The observation of a higher extent of the Ug and Tg substrates that are processed with a faster rate by the UE NEIL1 enzyme suggests that UE NEIL1 more effectively positions the Ug or Tg lesion in the active site in a manner that supports optimal base excision. In the recent structural study (Figure 3E,F), the

alternative quarantine conformation was observed only with Ed NEIL1.

NEIL1 Isoforms Differentially Recognize Uracil Glycol in Duplex DNA. Electrophoretic mobility shift assays (EMSA) were used to measure relative dissociation constants for the two NEIL1 isoforms to Ug- and Tg-containing duplex DNAs (Figure 4). EMSA were performed with the K54L





$\sim$			
C)	lesion	edited (nM)	unedited (nM)
	Ug:G	$11 \pm 1$	$16 \pm 3$
	Tg:G	$1.7 \pm 0.5$	$6.5 \pm 2.2$

Figure 4. Edited (Ed) NEIL1 binds to Tg- and Ug-containing DNAs tighter than the unedited isoform. Plot of percent bound enzyme, either Δ56 K54L Ed NEIL1 (blue) or Δ56 K54L UE NEIL1 (gray), vs total enzyme concentrations ([Etotal] =  $\sim$ [Efree]) for 30-nt duplexes (1•2) containing (A) Ug:G or (B) Tg:G measured by electrophoretic mobility shift assays (EMSAs). Panel (C) reports the values from EMSA and is shown in plots (A) and (B). Data was obtained at 25 °C and 150 mM NaCl with 10 pM substrate and enzyme concentrations ranging from 1000 to 0.2 nM. Data was fit to the equation:  $C[E]^n/((K_d)^n + [E]^n)$ , Hill coefficient = 1.

variant and truncated form of NEIL1 ( $\Delta 56$  K54L Ed NEIL1 and  $\Delta 56$  K54L UE NEIL1).  $^{32,37,40}$  Mutation of Lys54 to Leu ablates the NEIL1 glycosylase activity, allowing lesion-duplex affinity to be determined without substrate processing. Truncation of 56 residues from the disordered C terminal domain of NEIL1 improves the ability to resolve and quantify bands in the EMSA. Previous work has shown that this truncation does not significantly impact the activity of the enzyme. Both Ed and UE  $\Delta 56$  K54L NEIL1 display tight binding to Ug, with Ed NEIL1 binding slightly tighter (11  $\pm$  1 nM) than the unedited isoform (16  $\pm$  3 nM). The binding affinity of Ug:G is decreased relative to that of Tg:G (1.7  $\pm$  0.5 nM for Ed and 6.5  $\pm$  2.2 nM for UE NEIL1), 4 and the

magnitude of the affinity difference between the two isoforms is greater with Tg (Figure 4). Similarly, Ed  $\Delta$ 56 K54L NEIL1 exhibits an  $\sim$ 4-fold greater affinity (1.8  $\pm$  0.6 nM) than the unedited enzyme (6.3  $\pm$  0.2 nm) to a 5-OHU:G duplex.<sup>3</sup> Remarkably, the affinity is inversely correlated with substrate processing, where despite being more efficient at lesion removal, the UE NEIL1 isoform binds more weakly to Ug, Tg, and 5-OHU than edited NEIL1. The origin of base excision activity differences likely arises at catalytic steps and may be related to the amounts and positioning within the active site vs alternative sites. The inability to resolve multiple distinct binding modes in EMSA suggests that the affinities of the Ug lesion with the active site vs alternative sites are similar. Our data suggests that the affinity for these pyrimidine lesions may be slightly higher in the noncatalytic site, especially with Ed NEIL1, and this may serve to strategically control lesion excision.

UE NEIL1 Preferentially Removes Oxidized U/T Pyrimidine Lesions. UE NEIL1 was found to excise the oxidized lesions examined herein with the following trend in observed rates: Gh > Tg > Ug > 5-OHU > DHT > 5-OHC >  $OI \approx 5$ -hmU. The overall trend is similar but with some small differences for Ed NEIL: Gh  $\gg$  Ug > Tg > DHT  $\approx$  5-OHU > 5-OHC > OI  $\approx$  5-hmU. Notably, the relative difference in rate constants (UE/Ed) decreases as Tg > Ug > 5-OHU > 5-hmU  $\approx$  OI:C  $\geq$  DHT  $\approx$  OI:T > 5-OHC > Gh. From the NEIL1-Tg crystal structures and QM/MM calculations, Zhu et al. proposed that NEIL1 engages with the lactim tautomer of Tg to allow for hydrogen bonding of the Lys/Arg242 side chain with N3 of Tg (Figure S5). In this proposed mechanism, the differences in the p $K_a$  between UE (K242, p $K_a \sim 10.5$ ) and Ed (R242, p $K_a \sim 12.5$ ) provide for a greater extent of proton donation with UE NEIL1 to promote Tg tautomerization and facilitate faster excision.<sup>13</sup> Clearly, the influence of acidity of the 242 side chain is most dramatic with Tg, indicating that the contact may not occur or is less influential on NEIL1 excision with other pyrimidine lesions.

Gas-Phase Calculations Reveal Base Tautomerization Influences Base Excision. To provide insight into the mechanistic features of Ed and UE NEIL1 lesion-specific activities, we conducted gas-phase calculations of the pyrimidine lesions Tg, Ug, 5-OHU, 5-hmU, DHT, and 5-OHC, the purine lesion OI, and the lesion Gh, using B3LYP/6-31+G(d). Prior studies have shown that gas-phase calculations lend insight into the reactivity in the nonpolar environment of enzyme active sites. 41-46 Specifically, if the role of the glycosylase is to provide a hydrophobic environment, in which base lesion excision depends on the intrinsic lability of the N1-C1' bond, the gas-phase acidities have been shown to track, trendwise, with the rate of excision.

The five pyrimidine lesions, Tg, Ug, 5-OHU, 5-hmU, and DHT, can adopt lactim and lactam structures. 5-OHC lesion is a different structure from the other pyrimidines since it does not have a carbonyl at the 4 position and would not be defined as a lactam or lactim. The stability of the pyrimidine lesions in the lactam and lactim tautomeric forms was evaluated to provide insight into how the structure influences the intrinsic propensity to tautomerize. In the gas phase, we find that the most stable tautomer is the lactam, over the lactim, for Tg, Ug, 5-OHU, 5-hmU, and DHT (enthalpies in Table 3 and structures in Figure S6).

In terms of the relative stabilities among the lactim tautomers, for Tg, Ug, and 5-OHU, the 2-hydroxy lactim

Table 3. Relative Enthalpy of Lactam and Lactim Tautomers for NEIL1 Substrates

substrate	lactam	2-OH lactim <sup>b</sup>	4-OH lactim <sup>c</sup>
Tg	0.0	17.8:26.8	21.9:22.7
Ug	0.0	17.8:26.8	22.0:23.2
5-OHU	0.0	16.0:26.1	17.0:23.7
5-hmU	0.0	19.0:29.4	14.9:19.5
DHT	0.0	20.2:29.8	19.7:27.6

<sup>a</sup>All values are  $\Delta H$  at 298 K, calculated using B3LYP/6-31+G(d). <sup>b</sup>The first value is for the rotamer where the 2-OH proton is oriented toward the N3; the second value is for the proton oriented toward the N1. <sup>c</sup>The first value is for the 4-OH proton oriented toward the N3; the second value is for the proton oriented toward the C5.

("2-OH lactim") is preferred energetically. For 5-hmU and DHT, the 4-hydroxy lactim ("4-OH lactim") is more stable (Table 3 and Figure S6). Note that when each lactim is calculated, there are two possible rotamers. The 2-hydroxy group can have the proton oriented "toward" the N3 or "toward" the N1. Likewise, the 4-hydroxy proton could be pointed toward the N3 side of the substrate vs the C5. In actuality, this O-H bond may freely rotate, but when performing calculations, one has to "freeze" out the possible structures, as listed in Table 3. The calculations herein for Tg are in alignment with those previously reported, where Tg 2-OH lactim had a lower relative energy than the Tg 4-OH lactim tautomer. 13

The N1-H acidity ( $\Delta H_{\text{acid}}$ , kcal/mol) of the neutral more stable lactam substrates was determined to ascertain the correlation with the experimental trends for enzyme excision (Figure S6). We find that the calculated N1-H acidity trend for the lactam structures is 5-hmU (325.9) > 5-OHU (330.4) > Ug (341.4) > Tg (342.0) > DHT (347.7), which does not track with the trends observed in our experimental results (Table 1), either in the magnitude of excision rate constants  $k_g$ or in the UE:Ed NEIL1 excision rate ratio. This lack of correlation is consistent with the proposed importance of the lactim tautomer, which would be favored by the interaction with Lys242 in UE and Arg242 in the Ed NEIL1. 13

Given the proposed importance of the lactim structure in the excision mechanism, we also calculated the N1-H acidities for the 2-OH and 4-OH lactims (Figure S6). Regardless of whether we look at the 2-OH lactims or 4-OH lactims, none of the N1-H acidity trends track with either  $k_{\rm g}$  or the UE:Ed NEIL1 excision ratio (Table 1). For example, comparison of the 2-OH lactim tautomers in Figure S6 for the N1-H acidity of Tg vs 5-OHU shows that 5-OHU (acidity of 314.5 kcal/ mol) is much more acidic than Tg (acidity of 323.4 kcal/mol), but Tg has a faster excision rate constant  $k_g$  and higher UE:Ed NEIL1 excision rate ratio. Thus, the N1-H acidities of the lactims seem to show no correlation to experimental data.

N3 Proton Affinity Influences the Difference in Excision between the Two Isoforms. We determined the proton affinity (PA, kcal/mol) at N3 for the lactim forms of the pyrimidine lesions to evaluate the intrinsic propensity of N3 to behave as a hydrogen bond acceptor with Lys/Arg242 of NEIL1 (Figure S6). In initial calculations, we evaluated a model where all of the lesions adopt the 2-hydroxy form in the same rotamer, as proposed for Tg with NEIL1.<sup>13</sup> The N3 proton affinity trend is DHT (230.0, 2-OH lactim) > Tg (222.2, 2-OH lactim) > 5-hmU (220.4, 2-OH lactim) > Ug (219.5, 2-OH lactim) > 5-OHU (218.7, 2-OH lactim). This is

not consistent with the UE:Ed NEIL1 experimental excision ratio; this is not completely surprising in light of our calculations that showed that 5-hmU and DHT prefer the 4hydroxy lactim tautomer. Indeed, the tracking of the N3 proton affinity of the 2-hydroxy lactim for Tg, Ug, and 5-OHU and for the 4-hydroxy lactim for 5-hmU and DHT matches well with the experimental data: Tg(222.2, 2-OH lactim) > Ug(219.5, 2-OH lactim) > 5-OHU (218.7, 2-OH lactim) > 5hmU (215.2, 4-OH lactim) > DHT (214.7, 4-OH lactim). The three lesions that are more stable as the 2-hydroxy lactim form are also those that are most efficiently removed with the greatest preferential excision by UE over Ed NEIL1. This correlation between our calculations and the experimental excision ratio supports the importance of the N3 protonation with the most stable lactim.

Three lesions evaluated in this study are structurally different from the lactam/lactim pyrimidines: 5-OHC (a pyrimidine without a carbonyl at O4), Gh (guanidinohydantoin), and OI (a purine) (Figure S7). For 5-OHC, the analogous structure to the lactims would be the structures shown in Figure S7. Of these, the 5-OHC 4-NH lactim, with the 4-NH proton oriented toward N3, is the most stable lactim-like structure. Unlike the other pyrimidines, this structure has a proton on N3, which is not consistent with hydrogen bonding to the lysine or arginine in position 242. Due to this N3-H in 5-OHC, one might expect the edited form of NEIL1, with the less acidic R242, to render a faster excision rate than the UE; this is in fact found to be true (UE:Ed for 5-OHC is 0.7). The N3 has a relatively low PA as well of 174.4 kcal/mol. For Gh, the more stable lactim-like structure is Gh 2-OH lactim (here, we use atom numbering that is analogous to the pyrimidines) (Figure S7). This structure has a nitrogen that can hydrogen-bond to the lysine or arginine 242, but the proton affinity of that N3 is quite low (140.5 kcal/mol), presumably because Gh is already protonated, so another protonation would make the substrate doubly charged. Because Gh is charged, it is more quickly excised by both Ed and UE NEIL1(Table 1), consistent with the higher N1-H acidity (Figure S7); however, the UE/Ed excision ratio for Gh of 0.3 indicates that the more acidic K242 in the UE form does not enhance excision, which is also consistent with the low PA at N3. For OI, we also number the 6-membered ring like a pyrimidine. There are two possible lactims, with the more stable being the 4-OH lactim, whose PA at N3 is 206.0 kcal/mol. The ability of OI to more closely approximate a U/T lesion structure is consistent with the modest increased removal by UE over Ed.

The trend of the N3 PA for the most stable lactim and lactim-like structures for all of the lesions is as follows: Tg (222.2, 2-OH lactim) > Ug (219.5, 2-OH lactim) > 5-OHU (218.7, 2-OH lactim) > 5-hmU (215.2, 4-OH lactim) > DHT (214.7, 4-OH lactim) > OI (206.0, 4-OH lactim) > 5-OHC (174.4, 4-NH lactim) > Gh (140.5, 2-OH lactim) (Figure S8). This compares favorably to trends in the UE:Ed excision ratio (Table 1). Notably, the three pyrimidine lesions that are more stable as the 2-hydroxy lactim form are also those that are most efficiently removed with the greatest preferential excision by UE over Ed NEIL1. This correlation between our calculations and the experimental excision ratio supports the importance of the N3 proton affinity of the most stable lactim.

Insights into the Mechanism of Lesion-Specific Removal by Ed and UE NEIL1. Our experimental results and calculations suggest that pyrimidine lesions that are preferentially excised by UE NEIL1 more readily form the 2-

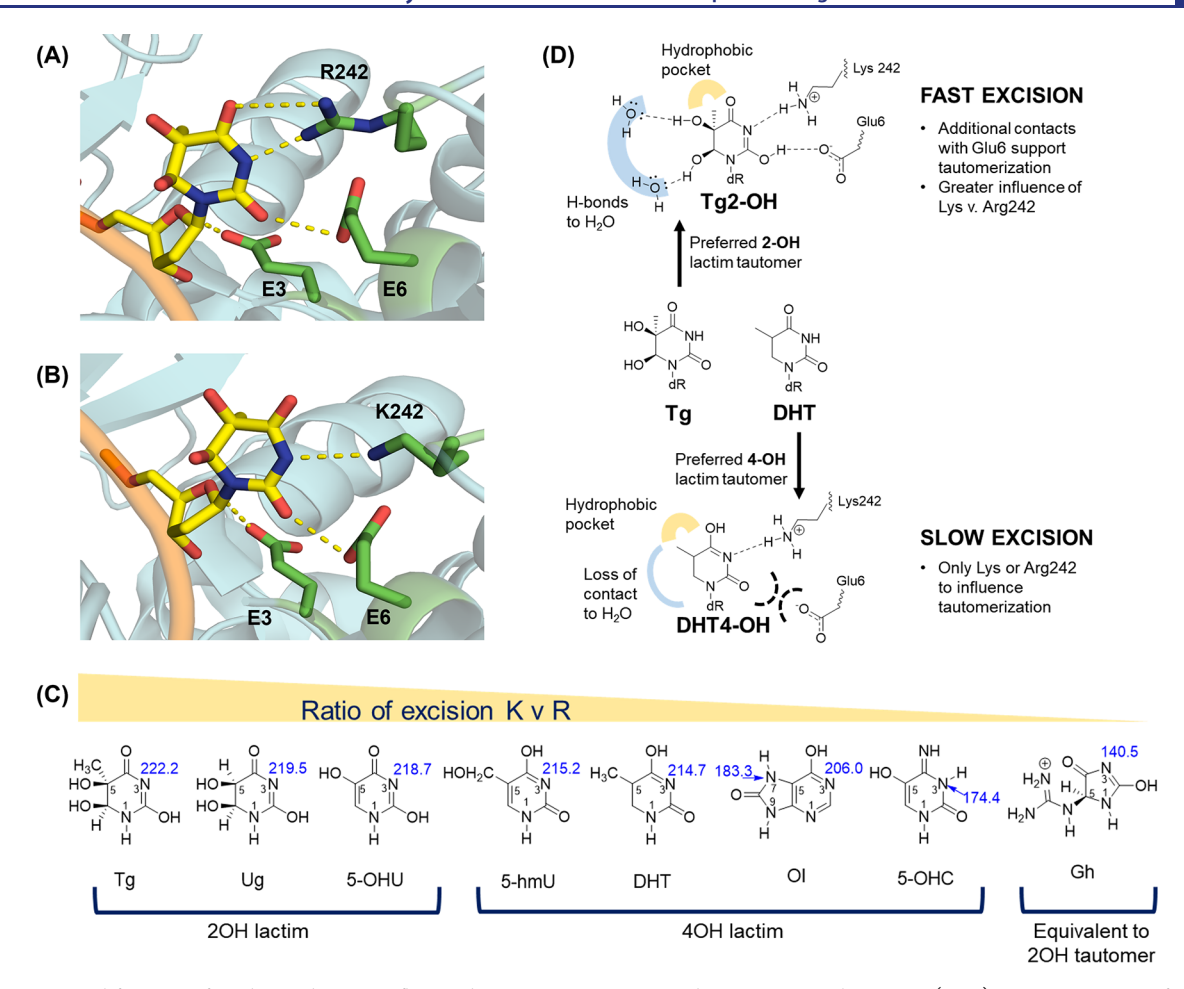


Figure 5. Structural features of oxidative damage influence base tautomerization and interaction with NEIL1. (A, B) X-ray structures of Ed (R242, PDB ID: SITY) and UE (K242, PDB ID:SITX) NEIL1 show that Glu3, Glu6, and Lys/Arg242 make key contacts with the Tg base. (C) Correlation of the ratio of the lesion excision and favored tautomer. Lesions are ordered based on N3 proton affinity ( $\Delta H$  kcal/mol, blue). The free base is shown as calculations were performed on free base, and excision rates were obtained with duplex DNA (Table 1). (D) Schematic proposal of the impact of the preferred base tautomer on the rate of excision and isoform difference excision.

OH lactim tautomer in the active site and therefore are readily protonated by Lys242 (Figure 5). The reduced N3 PA of lesions (5-hmU, DHT) that favor the 4-OH lactim tautomer likely makes the excision of these lesions less sensitive to the inherent differences in pKa of Lys vs Arg in UE and Ed NEIL1, respectively. Moreover, the lactim tautomer encountered by NEIL1 likely impacts placement in the activated conformation poised for catalysis relative to alternative or quarantine states. More favorable contacts between the catalytic residue Glu6 and the Tg 2-OH lactim tautomer were suggested on the basis of the Tg lesion-DNA structure. In contrast, the lesions that favor the 4-OH tautomer, such as DHT, may not provide for the preferred alignment of the catalytic residues with either isoform for optimal excision. The lesion-specific features are likely further exacerbated by the residue at position 242 and its influence on tautomerization and engagement within the active site. Indeed, in the structural studies, Arg242 in Ed NEIL1 was not engaged with the dihydrouracil (DHU) lesion and was pointed away in an alternate conformation (Figure 3E,F).

The activity of NEIL1 on Ug, which lacks the methyl group of Tg, revealed additional features that highlight the intricate relationship between lesion structure, binding and excision, and NEIL1 isoform. The magnitude of the preferred excision by UE over Ed NEIL1 decreased with Ug compared to that with Tg, which was consistent with the decreased N3 proton

affinity due to the absence of the methyl group. The X-ray structures (R242, PDB ID: 5ITY and K242, PDB ID: 5ITX) also showed that the 5-methyl group of Tg is tucked into a hydrophobic pocket and its presence likely facilitates placement in the activated catalytic state. Indeed, the biphasic kinetics of NEIL1 processing with Ug is consistent with two distinct excision processes and a larger fraction of Ug is processed at the slower rate compared to that of Tg, with both isoforms consistent with the absence of the methyl group leading to reduced engagement within the active site. In addition, the kinetics of Ug excision by UE NEIL1 showed more substrate excision associated with the faster process than with Ed NEIL1, while the K<sub>d</sub> measurements showed that Ed NEIL1 binds Ug DNA with a higher affinity than UE NEIL1. These results suggest that Ed NEIL1 may bind more of the Ug lesion tightly in a nonproductive conformation. Taken together, the subtle differences observed with Ug underscore how the isoform tips the balance between the various lesion binding modes.

Catalytic Vs Structural Lesion Verification. Our results reveal an intimate relationship between the NEIL1-mediated recognition of lesion structure and catalysis of base excision. Structural features of a given lesion will impact propensity for tautomerization and inherent lability, as well as whether the lesion preferentially engages in the "activated" vs quarantine

state(s). Both NEIL1 isoforms remove flat, aromatic lesions (DHT, OI, 5-OHU/C) less efficiently than nonplanar lesions (Gh/Sp/Tg), suggesting that flat lesions are more readily captured in the quarantine state by stacking on Tyr244 (Figure 3F). The quarantine state may also be less likely to bind hydrophilic lesions (Tg/Gh) that are capable of solventmediated interactions in the activated conformation (Figures

A role for promoting tautomerization rationalizes the relative processing of the pyrimidine substrates Tg/Ug/5-OHU by UE vs Ed NEIL1. Both 5-OHC and Gh are removed more efficiently by Ed NEIL1. In the case of 5-OHC, enhanced tautomerization would not aid in removal since this would place a proton at N3 and provide for a repulsive interaction with the more acidic Lys242. The hydantoin lesion Gh is a much better substrate for both Ed and UE NEIL1 than Tg, and this is due to its inherent lability (as reflected in N1-H acidity). In this case, Lys/Arg242 to the lesion may be important for positioning the lesion within the active site rather than base excision catalysis. It should also be noted that FapyG lesions are also good substrates for both isoforms of NEIL1, indicating potential other important factors in defining excision.<sup>34</sup>

A critical factor that has been largely overlooked that strongly influences NEIL1 excision is the base positioned opposite the lesion. Indeed, all lesions are more efficiently removed when base-paired with "C", suggesting that the interaction of Arg118 with C impacts the placement of the lesion base into the active site and may also hinder binding in alternative noncatalytic modes. Moreover, the identity of the residue at 242 likely impacts the conformational flexibility of the lesion recognition loop and influences initial damage detection and base-flipping steps. In the absence of the lesion, the lesion recognition loop adopts a completely different conformation.<sup>47</sup> Previous structural and computational studies have argued that the loop conformational flexibility explains the wide substrate scope of the Fpg/Nei family of glycosylases. 12,13,47-49 Clearly, additional structural and biophysical studies will be needed to sort out the complex means by which NEIL1 isoforms select and excise different lesions in different contexts and the influence of the residue at

Biological Implications of NEIL1 Recoding. Editing of the NEIL1 pre-mRNA impacts the function of NEIL1 in vitro, yet the biological role of having two isoforms of NEIL1 is still unclear. ADAR1 overexpression and transcriptome hyperediting are associated with cancer. Additionally, ADAR1 expression is upregulated under conditions associated with inflammation, a feature of both cancer initiation and progression. 16,52 Two examples showed that NEIL1 mRNA was completely edited in patients with lung cancer and multiple myeloma. 50,51

From one gene, RNA editing by ADAR1 gives two isoforms of NEIL1 with overlapping but altered substrate specificities. This suggests that RNA editing may play a unique regulatory role in responding to cellular conditions and the spectrum of DNA lesions formed under specific cellular conditions. Under normal cellular conditions, in a given cell type, there may be a balance of the two isoforms needed to handle the lesions present. Conditions of oxidative stress and inflammation resulting in the increased generation of oxidative lesions (like Gh) also upregulate ADAR1 expression, providing more Ed NEIL1 to cope with these types of lesions. 53,54 On the flip side, aberrant hyperediting by ADAR1 of NEIL1 leading to reduced

amounts of UE NEIL1 may erode the repair of oxidized pyrimidines (5-OHU, Tg) resulting in increased mutations, strand breaks, and genomic instability. Genomic instability drives oncogenic transformation, a feature that is also known to be associated with ADAR1 overexpression. 50,5

### ASSOCIATED CONTENT

## Supporting Information

The Supporting Information is available free of charge at https://pubs.acs.org/doi/10.1021/jacs.2c03625.

Supporting Information includes information regarding experimental details, materials and methods, as well as supporting data and tables; Figure S1, representative gel images of both qualitative isoforms of NEIL1 processing of a variety of base lesions; Figure S2, synthetic scheme for Ug phosphonamidite; Figure S3, production curves for the excision of the Ug:C, Ug:G, and Ug:A by both isoforms of NEIL1 with manual kinetics methods; Figure S4, one exponential production curves of Ug removal by NEIL1 measured by rapid quench; Figure S5, proposed reaction pathways for NEIL1; Figure S6, tautomers, acidity, and proton affinities of NEIL1 lesions; Figure S7, tautomers, acidity, and proton affinities of neutral NEIL1 substrates; Figure S8, N3protonated and O2-protonated tautomers, acidity, and proton affinities of NEIL1 substrates; Table S1, sequences used in glycosylase and binding studies; NMR spectra for Ug synthesis; and detailed coordinate information for base lesions (Tg, Ug, 5-OHU, 5-hmU, 5-OHC, OI, and Gh) (PDF)

# AUTHOR INFORMATION

# **Corresponding Authors**

Jeehiun K. Lee - Department of Chemistry and Chemical Biology, Rutgers, The State University of New Jersey, New Brunswick, New Jersey 08854, United States; Email: jeehiun@chem.rutgers.edu

Sheila S. David – Department of Chemistry, University of California, Davis, Davis, California 95616, United States; orcid.org/0000-0001-5873-7935; Email: ssdavid@ ucdavis.edu

### **Authors**

Elizabeth R. Lotsof – Department of Chemistry, University of California, Davis, Davis, California 95616, United States Allison E. Krajewski – Department of Chemistry and Chemical Biology, Rutgers, The State University of New Jersey, New Brunswick, New Jersey 08854, United States Brittany Anderson-Steele – Department of Chemistry,

University of California, Davis, Davis, California 95616, United States

JohnPatrick Rogers - Department of Chemistry, University of California, Davis, Davis, California 95616, United States

Lanxin Zhang - Department of Chemistry and Chemical Biology, Rutgers, The State University of New Jersey, New Brunswick, New Jersey 08854, United States

**Jongchan Yeo** – Department of Chemistry, University of California, Davis, Davis, California 95616, United States

Savannah G. Conlon – Department of Chemistry, University of California, Davis, Davis, California 95616, United States Amelia H. Manlove - Department of Chemistry, University of California, Davis, Davis, California 95616, United States

Complete contact information is available at: https://pubs.acs.org/10.1021/jacs.2c03625

# **Author Contributions**

§E.R.L., A.E.K., and B.A.S. contributed equally. The manuscript was written through contributions of all authors. All authors have given approval to the final version of the manuscript.

#### **Funding**

This work was supported by grants from the National Institutes of Health (GM143557 to SSD) and the National Science Foundation (JL). A.H.M. was a predoctoral trainee supported by T32-GM008799 and fellowships from GAANN and Corson-Dow to UC Davis. S.G.C. was supported by the Achievement Rewards for College Scientists (ARCS) fellowship.

#### Notes

The authors declare no competing financial interest.

### ACKNOWLEDGMENTS

The authors thank Dr. Chuan He (University of Chicago) for providing 5-fC, 5-caC, and 5-hmC containing oligonucleotides. Additionally, the authors thank Phil Yuen and Jonathan Ashby for help with the MS analysis of modified oligonucleotides and Joshua Bumgarner for creating the bar graphs in Figure 2.

#### ABBREVIATIONS

5-OHC
5-hydroxycytosine
5-caC
5-carboxycytosine
5-fC
5-formylcytosine
5-hydroxymethylcytosine
5-mC
5-methylcytosine
5-hydroxymethyluracil
5-OHU
5-hydroxymethyluracil
4
adenosine

ADAR1 adenosine deaminase acting on RNA 1

BER base excision repair

C cytosine
DHT dihydrothymine
DHU dihydrouracil
Ed edited
G guanosine

Gh guanidinohydantoin

EMSAs electrophoretic mobility shift assays
FapyA 4,6-diamino-5-formamido-pyrimidine
FapyG 2,6-diamino-4-oxo-5-formamidopyrimidine

FGh 2'F-guanidinohydantoin

Fpg formamidopyrimidine DNA glycosylase

FTg 2'-fluorothymidine glycol

I inosine

OG 8-oxo-7,8-dihydroguanine

OI 8-oxoinosine PA proton affinity

RONS reactive nitrogen and oxygen species

Sp spiroiminodihydantoin

T thymine

TET ten-eleven-translocation

Tg thymine glycol UE unedited Ug uracil glycol

#### REFERENCES

- (1) Lindahl, T. Instability and Decay of the Primary Structure of DNA. *Nature* **1993**, *362*, 709–715.
- (2) David, S. S.; Williams, S. D. Chemistry of Glycosylases and Endonucleases Involved in Base-Excision Repair. *Chem. Rev.* **1998**, *98*, 1221–1262.
- (3) Neeley, W. L.; Essigmann, J. M. Mechanisms of Formation, Genotoxicity, and Mutation of Guanine Oxidation Products. *Chem. Res. Toxicol.* **2006**, *19*, 491–505.
- (4) Sampath, H.; Batra, A. K.; Vartanian, V.; Carmical, J. R.; Prusak, D.; King, I. B.; Lowell, B.; Earley, L. F.; Wood, T. G.; Marks, D. L.; McCullough, A. K.; R Stephen, L. Variable Penetrance of Metabolic Phenotypes and Development of High-Fat Diet-Induced Adiposity in NEIL1-Deficient Mice. *Am. J. Physiol.: Endocrinol. Metab.* **2011**, 300, No. E724.
- (5) Vartanian, V.; Lowell, B.; Minko, I. G.; Wood, T. G.; Ceci, J. D.; George, S.; Ballinger, S. W.; Corless, C. L.; McCullough, A. K.; Lloyd, R. S. The Metabolic Syndrome Resulting from a Knockout of the NEIL1 DNA Glycosylase. *Proc. Natl. Acad. Sci. U.S.A.* **2006**, *103*, 1864–1869.
- (6) Chan, M. K.; Ocampo-Hafalla, M. T.; Vartanian, V.; Jaruga, P.; Kirkali, G.; Koenig, K. L.; Brown, S.; Lloyd, R. S.; Dizdaroglu, M.; Teebor, G. W. Targeted Deletion of the Genes Encoding NTH1 and NEIL1 DNA N-Glycosylases Reveals the Existence of Novel Carcinogenic Oxidative Damage to DNA. *DNA Repair* **2009**, *8*, 786–794.
- (7) Mori, H.; Ouchida, R.; Hijikata, A.; Kitamura, H.; Ohara, O.; Li, Y.; Gao, X.; Yasui, A.; Lloyd, R. S.; Wang, J. Y. Deficiency of the Oxidative Damage-Specific DNA Glycosylase NEIL1 Leads to Reduced Germinal Center B Cell Expansion. *DNA Repair* **2009**, *8*, 1328–1332.
- (8) Canugovi, C.; Shamanna, R. A.; Croteau, D. L.; Bohr, V. A. Base Excision DNA Repair Levels in Mitochondrial Lysates of Alzheimer's Disease. *Neurobiol. Aging* **2014**, *35*, 1293–1300.
- (9) Canugovi, C.; Yoon, J. S.; Feldman, N. H.; Croteau, D. L.; Mattson, M. P.; Bohr, V. A. Endonuclease VIII-like 1 (NEIL1) Promotes Short-Term Spatial Memory Retention and Protects from Ischemic Stroke-Induced Brain Dysfunction and Death in Mice. *Proc. Natl. Acad. Sci. U.S.A.* 2012, 109, 14948–14953.
- (10) Athanasiadis, A.; Rich, A.; Maas, S. Widespread A-to-I RNA Editing of Alu-Containing MRNAs in the Human Transcriptome. *PLoS Biol.* **2004**, *2*, No. e391.
- (11) Li, J. B.; Levanon, E. Y.; Yoon, J.-K.; Aach, J.; Xie, B.; Leproust, E.; Zhang, K.; Gao, Y.; Church, G. M. Genome-Wide Identification of Human RNA Editing Sites by Parallel DNA Capturing and Sequencing. *Science* **2009**, 324, 1210–1213.
- (12) Yeo, J.; Goodman, R. A.; Schirle, N. T.; David, S. S.; Beal, P. A. RNA Editing Changes the Lesion Specificity for the DNA Repair Enzyme NEIL1. *Proc. Natl. Acad. Sci. U.S.A.* **2010**, *107*, 20715—20719.
- (13) Zhu, C.; Lu, L.; Zhang, J.; Yue, Z.; Song, J.; Zong, S.; Liu, M.; Stovicek, O.; Gao, Y. Q.; Yi, C. Tautomerization-Dependent Recognition and Excision of Oxidation Damage in Base-Excision DNA Repair. *Proc. Natl. Acad. Sci. U.S.A.* **2016**, *113*, 7792–7797.
- (14) Onizuka, K.; Yeo, J.; David, S. S.; Beal, P. A. NEIL1 Binding to DNA Containing 2'-Fluorothymidine Glycol Stereoisomers and the Effect of Editing. *ChemBioChem* **2012**, *13*, 1338–1348.
- (15) Cao, S.; Rogers, J.; Yeo, J.; Anderson-Steele, B.; Ashby, J.; David, S. S. 2'-Fluorinated Hydantoins as Chemical Biology Tools for Base Excision Repair Glycosylases. *ACS Chem. Biol.* **2020**, *15*, 915–924.
- (16) Teoh, P. J.; An, O.; Chung, T. H.; Chooi, J. Y.; Toh, S. H. M.; Fan, S.; Wang, W.; Koh, B. T. H.; Fullwood, M. J.; Ooi, M. G.; de Mel, S.; Soekojo, C. Y.; Chen, L.; Ng, S. B.; Yang, H.; Chng, W. J. Aberrant Hyperediting of the Myeloma Transcriptome by ADAR1 Confers Oncogenicity and Is a Marker of Poor Prognosis. *Blood* **2018**, 132, 1304–1317.
- (17) Bandaru, V.; Sunkara, S.; Wallace, S. S.; Bond, J. P. A Novel Human DNA Glycosylase That Removes Oxidative DNA Damage

- and Is Homologous to Escherichia Coli Endonuclease VIII. DNA Repair 2002, 1, 517–529.
- (18) David, S. S.; O'Shea, V. L.; Kundu, S. Base-Excision Repair of Oxidative DNA Damage. *Nature* **2007**, 447, 941–950.
- (19) Krishnamurthy, N.; Zhao, X.; Burrows, C. J.; David, S. S. Superior Removal of Hydantoin Lesions Relative to Other Oxidized Bases by the Human DNA Glycosylase HNEIL1. *Biochemistry* **2008**, 47, 7137–7146.
- (20) Grin, I. R.; Zharkov, D. O. Eukaryotic Endonuclease VIII-like Proteins: New Components of the Base Excision DNA Repair System. *Biochemistry (Moscow)* **2011**, *76*, 80–93.
- (21) Jaruga, P.; Birincioglu, M.; Rosenquist, T. A.; Dizdaroglu, M. Mouse NEIL1 Protein Is Specific for Excision of 2,6-Diamino-4-Hydroxy-5- Formamidopyrimidine and 4,6-Diamino-5-Formamidopyrimidine from Oxidatively Damaged DNA. *Biochemistry* **2004**, *43*, 15909–15914.
- (22) Zhang, Q. M.; Yonekura, S. I.; Takao, M.; Yasui, A.; Sugiyama, H.; Yonei, S. DNA Glycosylase Activities for Thymine Residues Oxidized in the Methyl Group Are Functions of the HNEIL1 and HNTH1 Enzymes in Human Cells. DNA Repair 2005, 4, 71–79.
- (23) Minko, I. G.; Vartanian, V. L.; Tozaki, N. N.; Coskun, E.; Coskun, S. H.; Jaruga, P.; Yeo, J.; David, S. S.; Stone, M. P.; Egli, M.; Dizdaroglu, M.; McCullough, A. K.; Lloyd, R. S. Recognition of DNA Adducts by Edited and Unedited Forms of DNA Glycosylase NEIL1. DNA Repair 2020, 85, No. 102741.
- (24) Spruijt, C. G.; Gnerlich, F.; Smits, A. H.; Pfaffeneder, T.; Jansen, P. W. T. C.; Bauer, C.; Münzel, M.; Wagner, M.; Müller, M.; Khan, F.; Eberl, H. C.; Mensinga, A.; Brinkman, A. B.; Lephikov, K.; Müller, U.; Walter, J.; Boelens, R.; Van Ingen, H.; Leonhardt, H.; Carell, T.; Vermeulen, M. Dynamic Readers for 5-(Hydroxy)-Methylcytosine and Its Oxidized Derivatives. *Cell* **2013**, *152*, 1146–1159
- (25) Slyvka, A.; Mierzejewska, K.; Bochtler, M. Nei-like 1 (NEIL1) Excises 5-Carboxylcytosine Directly and Stimulates TDG-Mediated 5-Formyl and 5-Carboxylcytosine Excision. *Sci. Rep.* **2017**, *7*, No. 9001.
- (26) Schomacher, L.; Han, D.; Musheev, M. U.; Arab, K.; Kienhöfer, S.; Von Seggern, A.; Niehrs, C. Neil DNA Glycosylases Promote Substrate Turnover by Tdg during DNA Demethylation. *Nat. Struct. Mol. Biol.* **2016**, 23, 116–124.
- (27) Foksinski, M.; Rozalski, R.; Guz, J.; Ruszkowska, B.; Sztukowska, P.; Piwowarski, M.; Klungland, A.; Olinski, R. Urinary Excretion of DNA Repair Products Correlates with Metabolic Rates as Well as with Maximum Life Spans of Different Mammalian Species. *Free Radicals Biol. Med.* **2004**, *37*, 1449–1454.
- (28) Fleming, A. M.; Burrows, C. J. Formation and Processing of DNA Damage Substrates for the HNEIL Enzymes. *Free Radical Biol. Med.* **2017**, *107*, 35–52.
- (29) Kreutzer, D. A.; Essigmann, J. M. Oxidized, Deaminated Cytosines Are a Source of  $C \rightarrow T$  Transitions in Vivo. *Proc. Natl. Acad. Sci. U.S.A.* **1998**, 95, 3578–3582.
- (30) Purmal, A. A.; Kow, Y. W.; Wallace, S. S. Major Oxidative Products of Cytosine, 5-Hydroxycytosine and 5-Hydroxycracil, Exhibit Sequence Context-Dependent Mispairing in Vitro. *Nucleic Acids Res.* **1994**, *22*, 72–78.
- (31) Purmal, A. A.; Bond, J. P.; Lyons, B. A.; Kow, Y. W.; Wallace, S. S. Uracil Glycol Deoxynucleoside Triphosphate Is a Better Substrate for DNA Polymerase I Klenow Fragment Than Thymine Glycol Deoxynucleoside Triphosphate. *Biochemistry* **1998**, *37*, 330–338.
- (32) Doublié, S.; Bandaru, V.; Bond, J. P.; Wallace, S. S. The Crystal Structure of Human Endonuclease VIII-like 1 (NEIL1) Reveals a Zincless Finger Motif Required for Glycosylase Activity. *Proc. Natl. Acad. Sci. U.S.A.* **2004**, *101*, 10284–10289.
- (33) Porello, S. L.; Leyes, A. E.; David, S. S. Single-Turnover and Pre-Steady-State Kinetics of the Reaction of the Adenine Glycosylase MutY with Mismatch-Containing DNA Substrates. *Biochemistry* **1998**, 37, 14756–14764.
- (34) He, Y. F.; Li, B. Z.; Li, Z.; Liu, P.; Wang, Y.; Tang, Q.; Ding, J.; Jia, Y.; Chen, Z.; Li, N.; Sun, Y.; Li, X.; Dai, Q.; Song, C. X.; Zhang, K.; He, C.; Xu, G. L. Tet-Mediated Formation of 5-Carboxylcytosine

- and Its Excision by TDG in Mammalian DNA. Science 2011, 333, 1303-1307.
- (35) Maiti, A.; Drohat, A. C. Thymine DNA Glycosylase Can Rapidly Excise 5-Formylcytosine and 5-Carboxylcytosine: Potential Implications for Active Demethylation of CpG Sites. *J. Biol. Chem.* **2011**, *286*, 35334–35338.
- (36) Grin, I. R.; Dianov, G. L.; Zharkov, D. O. The Role of Mammalian NEIL1 Protein in the Repair of 8-Oxo-7,8-Dihydroadenine in DNA. *FEBS Lett.* **2010**, *584*, 1553–1557.
- (37) Yeo, J.; Lotsof, E. R.; Anderson-Steele, B. M.; David, S. S. RNA Editing of the Human DNA Glycosylase NEIL1 Alters Its Removal of 5-Hydroxyuracil Lesions in DNA. *Biochemistry* **2021**, *60*, 1485–1497.
- (38) Rogers, J. Creating a Chemical Toolbox: The Chemical Synthesis of Modified Nucleotides as Probes of DNA Repair Glycosylases. Ph.D. Dissertation, University of California, Davis, Davis, CA, 2007
- (39) Liu, M.; Zhang, J.; Zhu, C.; Zhang, X.; Xiao, W.; Yan, Y.; Liu, L.; Zeng, H.; Gao, Y. Q.; Yi, C. DNA Repair Glycosylase hNEIL1 Triages Damaged Bases via Competing Interaction Modes. *Nat. Commun.* **2021**, *12*, No. 4108.
- (40) Vik, E. S.; Alseth, I.; Forsbring, M.; Helle, I. H.; Morland, I.; Luna, L.; Bjørås, M.; Dalhus, B. Biochemical Mapping of Human NEIL1 DNA Glycosylase and AP Lyase Activities. *DNA Repair* **2012**, *11*, 766–773.
- (41) Michelson, A. Z.; Rozenberg, A.; Tian, Y.; Sun, X.; Davis, J.; Francis, A. W.; O'Shea, V. L.; Halasyam, M.; Manlove, A. H.; David, S. S.; Lee, J. K. Gas-Phase Studies of Substrates for the DNA Mismatch Repair Enzyme MutY. J. Am. Chem. Soc. 2012, 134, 19839–19850.
- (42) Maiti, A.; Morgan, M. T.; Drohat, A. C. Role of Two Strictly Conserved Residues in Nucleotide Flipping and N-Glycosylic Bond Cleavage by Human Thymine DNA Glycosylase. *J. Biol. Chem.* **2009**, 284, 36680–36688.
- (43) Morgan, M. T.; Bennett, M. T.; Drohat, A. C. Excision of 5-Halogenated Uracils by Human Thymine DNA Glycosylase: Robust Activity for DNA Contexts Other than CpG. *J. Biol. Chem.* **2007**, 282, 27578–27586.
- (44) Sun, X.; Lee, J. K. Acidity and Proton Affinity of Hypoxanthine in the Gas Phase versus in Solution: Intrinsic Reactivity and Biological Implications. *J. Org. Chem.* **2007**, *72*, 6548–6555.
- (45) Bennett, M. T.; Rodgers, M. T.; Hebert, A. S.; Ruslander, L. E.; Eisele, L.; Drohat, A. C. Specificity of Human Thymine DNA Glycosylase Depends on N-Glycosidic Bond Stability. *J. Am. Chem. Soc.* **2006**, *128*, 12510–12519.
- (46) Michelson, A. Z.; Chen, M.; Wang, K.; Lee, J. K. Gas-Phase Studies of Purine 3-Methyladenine DNA Glycosylase II (AlkA) Substrates. *J. Am. Chem. Soc.* **2012**, *134*, 9622–9633.
- (47) Duclos, S.; Aller, P.; Jaruga, P.; Dizdaroglu, M.; Wallace, S. S.; Doublié, S. Structural and Biochemical Studies of a Plant Formamidopyrimidine-DNA Glycosylase Reveal Why Eukaryotic Fpg Glycosylases Do Not Excise 8-Oxoguanine. *DNA Repair* **2012**, *11*, 714–725.
- (48) Jia, L.; Shafirovich, V.; Geacintov, N. E.; Broyde, S. Lesion Specificity in the Base Excision Repair Enzyme HNeil1: Modeling and Dynamics Studies. *Biochemistry* **2007**, *46*, 5305–5314.
- (49) Perlow-Poehnelt, R. A.; Zharkov, D. O.; Grollman, A. P.; Broyde, S. Substrate Discrimination by Formamidopyrimidine-DNA Glycosylase: Distinguishing Interactions within the Active Site. *Biochemistry* **2004**, *43*, 16092–16105.
- (50) Xu, L.; Di; Öhman, M. ADAR1 Editing and Its Role in Cancer. Genes 2019, 10, No. 12.
- (51) Anadón, C.; Guil, S.; Simó-Riudalbas, L.; Moutinho, C.; Setien, F.; Martínez-Cardús, A.; Moran, S.; Villanueva, A.; Calaf, M.; Vidal, A.; Lazo, P. A.; Zondervan, I.; Savola, S.; Kohno, T.; Yokota, J.; De Pouplana, L. R.; Esteller, M. Gene Amplification-Associated Overexpression of the RNA Editing Enzyme ADAR1 Enhances Human Lung Tumorigenesis. *Oncogene* 2016, 35, 4407–4413.
- (52) Rabinovici, R.; Kabir, K.; Chen, M.; Su, Y.; Zhang, D.; Luo, X.; Yang, J. H. ADAR1 Is Involved in the Development of Microvascular Lung Injury. *Circ. Res.* **2001**, *88*, 1066–1071.

- (53) Maydanovych, O.; Beal, P. A. Breaking the Central Dogma by RNA Editing. *Chemical Reviews*. American Chemical Society August 2006, pp 3397–3411. DOI: 10.1021/cr050314a.
- (54) Yang, J. H.; Luo, X.; Nie, Y.; Su, Y.; Zhao, Q.; Kabir, K.; Zhang, D.; Rabinovici, R. Widespread Inosine-Containing MRNA in Lymphocytes Regulated by ADAR1 in Response to Inflammation. *Immunology* **2003**, *109*, 15–23.
- (55) Bhate, A.; Sun, T.; Li, J. B. ADAR1: A New Target for Immuno-Oncology Therapy. *Molecular Cell*. Cell Press March 7, 2019, pp 866–868. DOI: 10.1016/j.molcel.2019.02.021.

# **□** Recommended by ACS

A Chemical Approach to Introduce 2,6-Diaminopurine and 2-Aminoadenine Conjugates into Oligonucleotides without Need for Protecting Groups

Mimouna Madaoui, Muthiah Manoharan, et al.

AUGUST 16, 2022 ORGANIC LETTERS

READ 🗹

Visualizing "Alternative Isoinformational Engineered" DNA in A- and B-Forms at High Resolution

Shuichi Hoshika, Millie M. Georgiadis, et al.

AUGUST 15, 2022

JOURNAL OF THE AMERICAN CHEMICAL SOCIETY

READ 🗹

Small Interfering RNAs Containing Dioxane- and Morpholino-Derived Nucleotide Analogues Show Improved Off-Target Profiles and Chirality-Dependent *In Vivo* Kno...

Armin Hofmeister, Sabine Scheidler, et al.

OCTOBER 12, 2022

JOURNAL OF MEDICINAL CHEMISTRY

READ 🗹

Template-Free Assembly of Functional RNAs by Loop-Closing Ligation

Long-Fei Wu, John D. Sutherland, et al.

JULY 26, 2022

JOURNAL OF THE AMERICAN CHEMICAL SOCIETY

READ 🗹

Get More Suggestions >